FEMS Microbiology Ecology, 97, 2021, fiaa253

doi: 10.1093/femsec/fiaa253
Advance Access Publication Date: 14 December 2020
Research Article

RESEARCH ARTICLE

Survival of the fittest: how the rice microbial community forces *Sarocladium oryzae* into pathogenicity

K. J. Peeters[1], K. Audenaert[2] and M. Höfte[1,*,†]

[1]Faculty of Bioscience Engineering, Laboratory of Phytopathology, Department of Plants and Crops, Ghent University, Coupure Links 653, B-9000 Ghent, Belgium and [2]Faculty of Bioscience Engineering, Laboratory of Applied Mycology and Phenomics, Department of Plants and Crops, Ghent University, Valentin Vaerwyckweg 1, B-9000, Ghent, Belgium

*Corresponding author: Laboratory of Phytopathology, Department of Plants and Crops, Faculty of Bioscience Engineering, Ghent University. Coupure Links 653, 9000 Gent, Belgium. Tel: +32 9 2646017; E-mail: monica.hofte@ugent.be

One sentence summary: The success of the sheath rot pathogen *Sarocladium oryzae* is determined by its ability to withstand bacterial antagonists in the rice endosphere.

Editor: Paolina Garbeva
†M. Höfte, http://orcid.org/0000-0002-0850-32499

ABSTRACT

The fungus *Sarocladium oryzae* (Sawada) causes rice sheath rot and produces the phytotoxins cerulenin and helvolic acid. Both toxins show antimicrobial activity but only helvolic acid production in the rice sheath correlates with virulence. *Sarocladium oryzae* isolates that differ in their toxin production were used to study their interaction with the rice culturable bacterial endophyte community. The diversity and community structure was defined in the edge of sheath rot lesions, followed by a null model-based co-occurrence analysis to discover pairwise interactions. Non-random pairs were co-cultured to study the nature of the interactions and the role of the toxins herein. Compared to healthy sheaths, endophyte diversity strongly increased when infected with the least virulent *S. oryzae* isolates producing low amounts of toxins. Virulent *S. oryzae* isolates did not affect diversity but caused strong shifts in species composition. The endophyte community of healthy rice plants was dominated by *B. cereus*. This bacterium was enriched in lesions produced by low-virulent *S. oryzae* isolates and caused hyphal lysis. Contrarily, helvolic acid producers eliminated this bacterium from the sheath endosphere. We conclude that *S. oryzae* needs to produce antibiotics to defend itself against antagonistic rice endophytes to successfully colonize and infect the rice sheath.

Keywords: sheath rot; *Oryza sativa*; helvolic acid; cerulenin; diversity; endophytes

INTRODUCTION

Sarocladium oryzae is the major fungal sheath rot pathogen (Bigirimana *et al.* 2015). It has been reported in 36 countries (CABI 2020) and causes greyish-brown necrotic lesions on the uppermost leaf sheath enclosing the youngest panicle. In case of severe infection, which often occur in warm and humid conditions, grain production is affected and yield losses reach up to 85% (Sakthivel 2001; Panda and Mishra 2019). Sheath rot affects all growth stages but the most severe infections have been reported at booting stage (Pearce, Bridge and Hawkworth 2001). *Sarocladium oryzae* is mainly seed-borne and colonizes the

Received: 11 August 2020; **Accepted:** 10 December 2020

rice seedlings from the embryo, the endosperm or the hull where it resides (Dugay, Manandhar and Mew 1996). It also survives in soil, on plant residues and in other *Poaceae* (Sreenivasaprasad and Johnson 2001; Ayyadurai *et al*. 2005; Hittalmani *et al*. 2016). The fungus is often transmitted by insects such as stem borers, leafhoppers and mites (Dugay, Manandhar and Mew 1996; Pearce *et al*. 2001). The genus *Sarocladium* contains mainly endophytes that are associated with members of the *Poaceae* (Yeh and Kirschner 2014; Liu 2017; Anjos *et al*. 2020) among which the grass endophyte, *Sarocladium brachiariae*, to which *S. oryzae* closely relates (Liu 2017; Ou, Lin and Chen 2020). The genus also contains saprobes, mycoparasites, opportunistic human pathogens and plant pathogens (Giraldo *et al*. 2015; Anjos *et al*. 2020).

The main virulence factors of *S. oryzae* are cell wall degrading enzymes and the toxins cerulenin and helvolic acid (Ayyadurai *et al*. 2005; Peeters *et al*. 2020). Helvolic acid is a tetracyclic triterpenoid, produced by various plant endophytic fungi among which the *Anoectochilus setaceus* endophyte, *Xylaria* sp. (Tschen *et al*. 1997; Ratnaweera *et al*. 2014), the entomopathogenic fungus *Metarhizium anisopliae* and the opportunistic human pathogen *Aspergillus fumigatus* (Hittalmani *et al*. 2016). The toxin causes chlorosis in *Poaceae* and its production in the rice sheath is positively correlated with virulence (Tschen *et al*. 1997; Sakthivel, Amudha and Muthukrishnan 2002; Ayyadurai *et al*. 2005; Peeters *et al*. 2020). In addition to its phytotoxicity, helvolic acid shows antimicrobial activity, mainly against Gram-positive bacteria, by inhibiting protein biosynthesis and ATPase pumps (Tanaka, Kinoshita and Masukawa 1969; Yoshimura 1978). The hexaketide amide, cerulenin, is a dual-purpose toxin too. It inhibits the fatty acid and polyketide biosynthesis in plants and other microorganisms, especially in fungi (Omura 1976; Wenzel *et al*. 2011).

In previously published work, we showed that *S. oryzae* can be divided into three groups that differed in virulence and toxin production *in vitro* and *in planta* (Peeters *et al*. 2020). The isolates clustering with CBS 180.74 (Group 1) were the least pathogenic and produced the highest levels of cerulenin in culture. Isolates that clustered with CBS 399.73 (Group 2) were mainly low cerulenin producers and for some isolates, no cerulenin was detected at all. The third lineage clustered with strain CBS 414.81 (Group 3) and was far the most virulent on the *Japonica* cv Kitaake (Peeters *et al*. 2020). Helvolic acid production in culture did not correlate with lineage and the production *in vitro* did not correspond to the production *in planta* (Peeters *et al*. 2020). This was attributed to the phenotypic instability of the *S. oryzae* isolates, a process called sectorization. Isolates of the least virulent lineages (Group 1 and 2) showed sectorization under stressed conditions which resulted in a reduced helvolic acid production *in planta*. The most pathogenic lineage (Group 3) showed no sectorization in culture and maintained high helvolic acid production in the rice sheath (Peeters *et al*. 2020). Next to phenotypic instability, a decreased toxin production and hypovirulence, could be explained by a mycovirus infection (Nuss 2005; Santos *et al*. 2017). Transmission rates of mycoviruses are higher *in planta* than *in vitro* (Brusini and Robin 2013)., which could explain the reduced toxin levels in planta.

During infection, pathogens simultaneously need to cope with host defence responses and with microbial antagonists (Duffy, Schouten and Raaijmakers 2003). In the endosphere, they need to compete for nutrients and space with the established endophyte community. Endophytes are bacteria and fungi that colonize the intercellular space and the vascular system asymptomatically (Bacon and Hinton 2006; Mano and Morisaki 2008; Hardoim *et al*. 2012). They are often able to enhance biotic stress tolerance both indirectly and directly, by respectively inducing systemic resistance or by producing toxic chemical compounds, degrading virulence factors or predating on the pathogen (Whipps 2001; Laforest-Lapointe *et al*. 2017). Hosts harboring a diverse microbial community, have been reported to be more resistant against pathogen attack (Reiter *et al*. 2002; Ardanov *et al*. 2011). Consequently, the endosphere is considered a source of potential biocontrol agents and current literature focusses on the microbiome diversity and is biased towards screening for beneficial microbes (Yang, Crowley and Menge 2001; Cottyn *et al*. 2009; Bertani *et al*. 2016). The diversity of the rice endophyte community of the seeds, roots and shoots of rice has thus been well characterized by culture-dependent (Okunishi *et al*. 2005; Mano *et al*. 2007; Hardoim *et al*. 2012) and -independent techniques (Bertani *et al*. 2016; Musonerimana *et al*. 2020). The Gram-negative genera *Methylobacterium* (Elbeltagy *et al*. 2000; Mano *et al*. 2007; Bertani *et al*. 2016), *Burkholderia* (Yang, Crowley and Menge 2001; Bertani *et al*. 2016) and *Pantoea* (Yang, Crowley and Menge 2001; Mano *et al*. 2007; Bertani *et al*. 2016) are often reported in the shoots of rice and *Bacillus* is one of the most abundant Gram-positive genera in the rice root, straw and seed endosphere (Yang, Crowley and Menge 2001; Bertani *et al*. 2016). Because of this antagonism towards invaders, pathogens developed mechanisms to manipulate the microbial community of the host (Rovenich, Boshoven and Thomma 2014). They can detect microbes in their environment and respond by, amongst others, producing antimicrobial compounds or by activating efflux pumps that extrude toxic compounds produced by other microorganisms (Vorholt 2012; Kombrink and Thomma 2013; Deveau *et al*. 2018). These antimicrobial compounds often have dual-use and play a role in the interaction with the host and with the microbial environment. For example, LysM effectors are chitin-binding proteins that offer protection against chitinases that are produced by both microbial competitors and the host plant (Kombrink and Thomma 2013; Rovenich, Boshoven and Thomma 2014). Also fuscopeptins, lipodepsipeptides produced by the sheath rot pathogens *Pseudomonas fuscovaginae*, are used in the interaction with other microbes and with the host plants, rice (Coraiola *et al*. 2008).

The dual function of cerulenin and helvolic acid indicates that they also play a role in the interaction of *S. oryzae* with the microbial environment, both when associated with its host as in its free-living stage (Kombrink and Thomma 2013). Moreover, we hypothesize that the defence against other microbes is an important function of these toxins. While cerulenin is well known for its antibiotic characteristics (Porrini *et al*. 2014), there is still no evidence for its role in the infection of rice (Peeters *et al*. 2020). The fact that helvolic acid is also produced by endophytes (Tschen *et al*. 1997; Ratnaweera *et al*. 2014) and opportunistic animal pathogens (Hittalmani *et al*. 2016) supports this hypothesis since these organisms have in common that they need to persist in a hostile microbial environment. It is well known that *S. oryzae* shows antagonistic activity against *Bacillus subtilis*, an inhabitant of the rice endosphere and phyllosphere (Mano *et al*. 2007; Yang *et al*. 2008; Cottyn *et al*. 2009). This interaction has been used to quantify helvolic acid production *in vitro* (Ghosh *et al*. 2002) and to study the mode of action of cerulenin (Porrini *et al*. 2014). The increasing awareness that these interactions shape the host microbial community and determine the outcome of the infection, led to the concept 'pathobiome'. This is the totality of microbes interacting with a pathogen (Vayssier-Taussat *et al*. 2014; Jakuschkin *et al*. 2016).

As *S. oryzae* colonizes rice plants endophytically, from the seeds or introduced by insects, this study investigates the effect

of *S. oryzae* infection on the rice sheath endosphere bacterial community and the role of cerulenin and helvolic acid herein. With this, we aim to understand why *S. oryzae* produces cerulenin and helvolic acid. In addition, we investigate the importance of taking the population diversity of pathogens into account when studying microbial ecology. As the production of cerulenin and helvolic acid is variable, we hypothesize that the effect of sheath rot infection on the endophyte community is *S. oryzae* isolate-dependent (Peeters *et al.* 2020).

MATERIAL AND METHODS

Plant material and growth conditions

For the isolation of bacterial endophytes from *S. oryzae*-infected rice sheaths, 7 weeks-old plants of the *japonica* type rice (*Oryza sativa* L.) cv Kitaake were grown as described before (Peeters *et al.* 2020). Briefly, after sterilization of the rice seeds with 2% sodium hypochlorite, seeds were germinated in Petri dishes on moistened, sterile filter paper (Whatmann, grade 3). After 7 days of incubation, seedlings were planted per six in perforated plastic trays (22 × 15 × 6 cm) containing potting soil (Structural; Snebbout, Kaprijke, Belgium). For another 6 weeks, plants were grown in a glasshouse at 28°C at 60% relative humidity (RH) and were watered six times a day with a flooding system. Every week, the plants were supplemented with 0.2% iron sulphate and 0.1% ammonium sulphate.

Sarocladium oryzae isolates: storage, growth and rice inoculation

This study used *S. oryzae* isolates of which the toxin production on potato dextrose agar (PDA, Difco, VWR, Leuven, Belgium) plates and in the rice sheath has been described before (Peeters *et al.* 2020). An overview of the characteristics of the *S. oryzae* isolates used in this study is shown in Table 1. Pure cultures were stored at −80°C in 20% glycerol. Before use, isolates were taken from the collection and grown in the dark at 28°C for 1 week on PDA after which they were transferred to new PDA plates and grown for another 2 weeks in the same conditions. The standard grain inoculum technique was used to inoculate rice plants (Sakthivel and Gnanamanickam 1987). For this, one fully colonized rice grain was placed in the axil of the second youngest leaf. Healthy control plants were inoculated with a sterile rice grain. Both the preparation of the inoculum and the inoculation procedure are described in detail by Peeters *et al.* (2020). The inoculated plants were incubated under growth chamber conditions (28°C, 12h:12h light: dark, 85% RH during the first 24 h and 65% RH during days 2–11).

Isolation of endophytic bacteria

To obtain endophytic bacteria from infected rice plants, samples were collected from the rice sheath when the disease was fully established (8–11 days after inoculation). For this, 1 cm pieces from the edge of the lesion were collected and sterilized for 2 min in 70% ethanol followed by three rounds of rinsing in sterile distilled water. To isolate the endophytic bacteria, samples were homogenized for 60 s in 0.85% sterile saline solution and fine sand (river sand 0/2; Bouwpunt, Ghent, Belgium) that was autoclaved twice in 48 h. A 10-fold serial dilution of the crushed samples was plated on King's B agar (KB; King, Ward and Raney 1954), R2A agar (Fischer Scientific, Merelbeke, Belgium) and Mannitol Egg Yolk Polymyxin Agar (MYP) selective agar (Fischer Scientific, Merelbeke, Belgium) to avoid culturing biases. Plates were incubated in the dark at 28°C for 20–48 h and individual bacterial colonies were counted. Morphologically distinct (based on size, color, form and texture) bacterial isolates were selected, purified and stored at −80°C in 20% glycerol.

Phylogenic analysis

Starting from 24-hour-old cultures of the purified bacteria, a colony PCR was used to amplify the 16S region with the primers 16F27 (5'- AGAGTTTGATCMTGGCTCAG -3') and 16R1492 (5'- TACGGYTACCTTGTTACGAGTT -3'; Yakimov *et al.* 2003). An overview of the thermal profile is shown in Table S1 (Supporting Information). The amplicons were separated by horizontal electrophoresis using 1.5% agarose gels in TAE-buffer at 100 V for 25 min. In case no band was detected after using colony PCR, total genomic DNA was extracted using the Wizard Genomic DNA Purification kit (Promega, Leiden, The Netherlands) before amplifying the 16S region. PCR products were purified and sequenced by LGC Genomics GmbH (Berlin, Germany) using Sanger sequencing. Consensus sequences were generated with BioEdit version 7.2.5 and blasted against GenBank. Sequences of the most related species were retrieved from Genbank (Table S2, Supporting Information) and added to the analysis. For the multiple alignment, the MUSCLE algorithm (Edgar 2004) was applied and further phylogenic analysis was performed with MEGA6 (Tamura *et al.* 2013). The maximum-likelihood algorithm with 1000 replicates was used for phylogenetic tree construction. Based on the output of the phylogenetic analysis, the bacterial isolates were grouped into 19 operational taxonomic units (OTUs). Table S3 (Supporting Information) provides the accession numbers of the sequences generated during this study.

Dual plate assay and microscopy

In vitro antagonism was tested with a dual culture assay. A total of five *S. oryzae* isolates were grown together with ten bacterial isolates in a dual plate assay. The bacterial isolates represented the four OTUs that were significantly associated with at least one of the *S. oryzae* isolates according to the Pairs analysis. For this, a plug (Ø 6 mm) from the edge of a 2-weeks-old fungal colony was placed in the centre of a round Petri dish (Ø 9 cm, Novolab, Geeraardsbergen, Belgium) filled with PDA. Each species combination was repeated thrice. After 48 h of incubation at 28°C, bacteria from a 24-hour-old colony were streaked on both sides of the fungal colony at 2 cm distance from the centre of the fungal plug. The following 19 days, the interaction was monitored by measuring the bacterial inhibition zone and the fungal colony diameter. At 19 days after co-culturing the organisms, the interaction was evaluated microscopically according to the agar block smear preparation technique (Woo *et al.* 2010).

Statistical analysis

The statistical analyses were performed in R-4.0.0 (R Core Team 2020) and the FORTRAN software Pairs (Ulrich 2008). Before any further analysis, all bacterial counts were log-transformed. In case data were censored, non-detects were replaced by regression on order statistics (ROS) by use of the package NADA-1.6–1.1 (Helsel 2005). To avoid exclusion of conditions from the analysis, the data of conditions where all data were below the detection limit were estimated by ROS with the limit of detection (LOD) as the maximum value and LOD/4 as the minimum value. The

Table 1. Characteristics of the *S. oryzae* isolates used in this study as reported by Peeters *et al.* (2020).

	Helvolic acid		Cerulenin			Phylogenic group		
S. oryzae isolate	In vitro (μg/L)	In planta (μg/g)	In vitro (μg/L)	In planta (μg/g)	Lesion area (mm^2)	Peeters *et al.* (2020) [1]	Ou, Lin and Chen (2020) [2]	Sectorization
IBNG0008	126	5306	1402	58	236	Group 3	*S. sparsum*	–
BDNG0025	155	3892	16	5	227	Group 3	*S. sparsum*	–
RFRG2	0	0	982	1196	60	Group 1	*S. oryzae*	+
RFNG41	164	461	55	1	50	Group 2	*S. attenuatum*	+
RFNG30	0	2.2	0	0	38	Group 2	*S. attenuatum*	–

[1]Maximum-likelihood analysis based on the partial actin-gene (ACT) and the internal transcribed spacer region (ITS),
[2]Based on Maximum-likelihood analysis with ACT, ITS, the partial large ribosomal subunit (LSU) and the partial beta tubulin gene (TUB2), Ou, Lin and Chen (2020) have proposed to reclassify *S. oryzae* in three species, which correspond with the three groups that were described by Peeters *et al.* (2020).

output of this imputation analysis was further processed as non-censored data. Pairwise and multiple comparison analysis were performed with the packages lme4 v1.1–23 (Bates *et al.* 2015), car-3.0–7 (Fox and Weisberg 2019), afex-0.27–2 (Singmann *et al.* 2020), emmeans-1.4.6 (Lenth 2020), dunn.test-1.3.5 (Dinno 2017). Results of the parametric and non-parametric statistics used in this study are shown in the Tables S4–S7 (Supporting Information).

To analyse the composition of the bacterial communities, a non-metric multidimensional scaling (NMDS) with 1000 iterations, based on a Euclidean dissimilarity matrix (rows as samples, columns as species) of the individual samples, was performed using the R package vegan-2.5–6 (Oksanen *et al.* 2019). As external factors, the concentrations of cerulenin and helvolic acid in the rice sheath and on PDA, reported by Peeters *et al.* (2020) were added to the NMDS. Based on the transposed binary matrix, the species co-occurrence patterns were examined by use of a null model analysis with the R package EcoSimR-0.1–0 (Gotelli, Hart and Ellison 2015). The overall community C-score was computed and compared to the 95% confidence interval of the simulated scores of 1000 randomized null models that were generated using the fixed rows (species or OTUs)—fixed columns (samples) algorithm (sim9). To test for non-random pairwise associations among the isolates, we used the software Pairs (Ulrich 2008) to calculate the C-score and the togetherness (T-score) for each possible species pair. Pairs used a presence-absence based null model analysis for randomization with fixed row and column constraints, independent swap algorithm (200 iterations, 6210 swaps) to detect significantly aggregating or segregating species pairs. The output values of the Pairs analyses are Z-transformed ((score $_{observed}$—score $_{expected}$)/standard deviation)) scores that were corrected according to the BY criterion (Yaov and Yekuteli 2001) to reduce type I error rates. Aggregation corresponds to positive T-scores and negative C-scores, while the opposite is true for segregation.

RESULTS

Characterization of the bacterial endophyte community in sheath rot lesions

To investigate if the toxins cerulenin and helvolic acid affect the rice phyllosphere during infection, rice plants cv. Kitaake were inoculated with *S. oryzae* isolates with various levels of virulence and *in planta* toxin production (Figures S1 and S2, Supporting Information; Table 1). The group 3 isolates IBNG0008 and BDNG0025, produce high amounts of helvolic acid and have a significantly higher pathogenic potential. In cultures of the group 2 isolate RFNG41, similar concentrations of helvolic acid were measured but its toxin production was substantially lower in the rice sheaths, as was its virulence. The least pathogenic group 2 isolate RFNG30 produced no helvolic acid (Figures S1 and S2, Supporting Information; Table 1).

The culturable bacterial community was selected as a representative subgroup to study these biotic interactions. In two independent experiments, bacterial endophytes were isolated from surface-sterilized rice sheath fragments containing the edge of 8-days-old sheath rot lesions. In the first experiment, toxin production was confirmed by measuring cerulenin and helvolic acid levels in an 8 cm region containing the lesion (Figure S2, Supporting Information). In both experiments, sheath samples of each condition were plated on PDA to confirm the presence of the inoculated fungal isolate. *Sarocladium oryzae* isolate RFNG30, which produced only trace amounts of the toxins *in vitro* and in the rice sheath (Table 1 and Figure S2, Supporting Information), was overgrown by bacteria. During isolation of the toxin-producers BDNG0025 and IBNG0008, on the other hand, almost no other organisms grew out of the surface-sterilized sheath rot lesions except for one bacterium which was found closely associated with the virulent isolate IBNG0008. This bacterium was isolated and characterized as *Stenotrophomonas maltophilia*. One of the isolates was used further in the study and named A-0008-IB1 (Fig. 1).

A bacterial suspension, extracted from crushed sheath samples, was spread on different culture media (R2A, KB), minimizing cultural bias. To obtain maximal species richness, 54 bacterial colonies were selected based on morphological differences and identified by sequencing their 16S partial gene sequence. Maximum likelihood phylogenic analysis clustered the bacterial isolates in 19 operational taxonomic units (OTUs; Fig. 1). The majority of the bacterial isolates were Gram-positive bacteria, belonging to the genera *Bacillus*, *Brevibacillus* and *Paenibacillus*. Of the Gram-negative bacteria, *S. maltophilia* was the most abundant species (Fig. 1). With 10 OTUs in the first experiment and six OTUs in the second, the most diverse bacterial community was found in the lesions of the *S. oryzae* isolate RFNG30 with a Shannon index (H) of respectively $H = 1.76$ and $H = 1.59$ (Fig. 1). This isolate produces no helvolic acid at all (Table 1 and Figure S2, Supporting Information). Sheath rot lesions, caused by the low helvolic acid producer RFNG41, had a slightly less diverse community ($H = 1.13$) of which five OTUs were isolated (Fig. 1). Healthy plants ($H = 0.49$ and $H = 0.35$) and plants infected by the high helvolic acid producers, IBNG0008 ($H = 0.57$ and $H = 0.31$) and BDNG0025 ($H = 0.45$), had a less diverse bacterial endophyte community. From healthy rice sheaths, three OTUs were

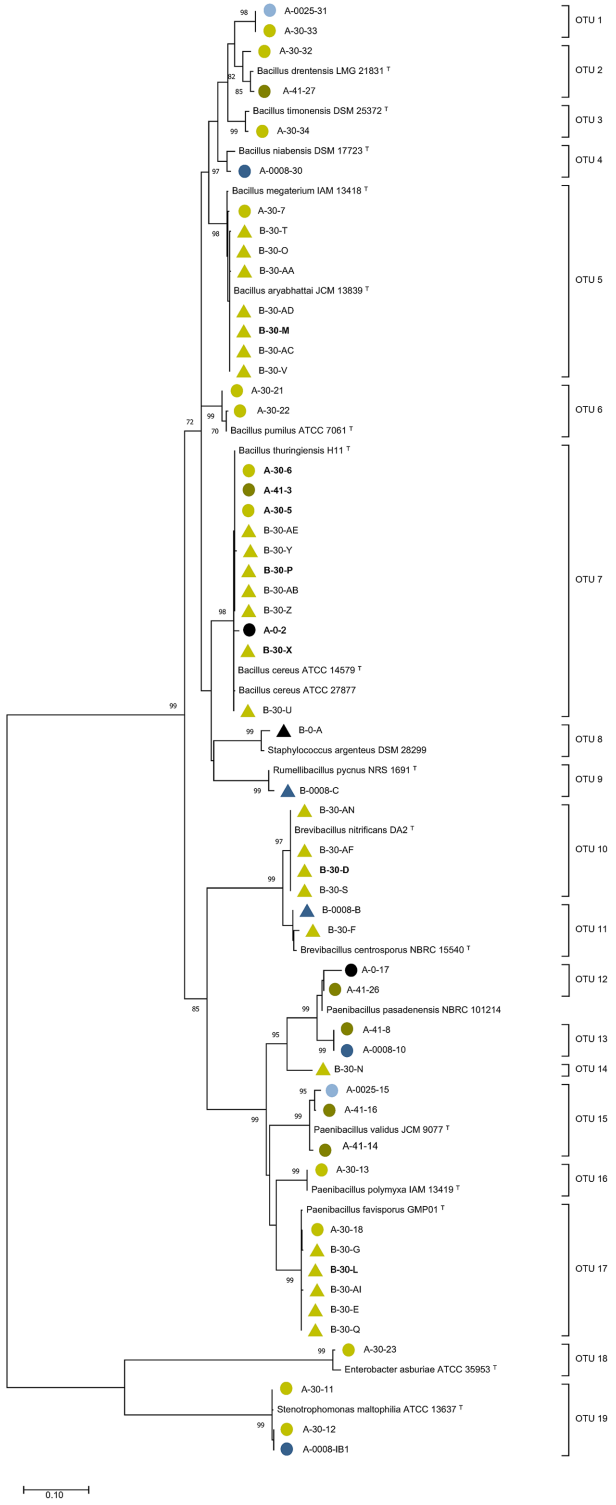

Figure 1. Phylogenic tree based on the partial 16S gene sequence of bacterial isolates from the rice phyllosphere and their closest phylogenic relatives. At 8 days post-inoculation of *Saroclaudium oryzae* isolates IBNG0008 (dark blue), BDNG0025 (light blue), RFNG41 (dark green) or RFNG30 (light green), rice sheath samples were collected and bacterial endophytes were isolated and identified based on their 16S sequence. Bacteria isolated from healthy rice sheaths are represented by black symbols. The experiment was performed twice, marked by circles (●) or triangles (▲). Bacteria in bold were used in the dual plate assay

isolated in total and from the plants inoculated with the virulent, toxin-producing *S. oryzae* isolates IBNG0008 and BDNG0025 respectively five OTUs and two OTUs (Fig. 1).

Co-occurrence analysis implementing the toxins helvolic acid and cerulenin

A non-metric multidimensional analysis (NMDS) that included the *S. oryzae* isolates visualizes how sheath rot infection resulted in different bacterial communities depending on the isolate (Fig. 2). A stable, three-dimensional NMDS ordination was reached after 20 restarts with a stress value of 0.0135. In the ordination plot, symbols represent the samples of both experiments. Samples with similar species composition are positioned close together. The NMDS shows that the bacterial community of the healthy control plants takes a central position in the ordination plot. Samples infected with the least pathogenic isolate (RFNG30), which produces no toxins, cluster together. Samples infected with the toxin-producers are located on the other side of the NMDS plot (Fig. 2). The grey vectors on the NMDS ordination plot show the species that were significantly ($P < 0.01$) correlated to the ordination (Fig. 2). Species vectors pointing in the same direction indicate species with similar distributions while opposite vectors indicate species that do not tend to co-occur. Null model analysis of species co-occurrence showed that the observed c-score of the overall community (6.28) was significantly higher than the mean simulated c-scores of the null models (5.58 ± 0.02). This indicates that the species distribution over the different samples follows a non-random, segregated assemblage structure (matrix SES = 5.36; Figure S3, Supporting Information). Table 2 shows the species pairs that associate (togetherness score) or segregate (c-score) according to a pairwise analysis. All species pairs were analysed but only the ones showing significant non-random associations ($P < 0.05$) are listed (Table 2). The analysis confirmed that OTU 5, 7 and 17 did not co-occur with the *S. oryzae* isolate IBNG0008 while OTU 5, 7, 10 and 17 significantly aggregated with *S. oryzae* RFNG30 (Table 2). No significant species pairs were formed with the remaining two *S. oryzae* isolates. Plants were only in the first experiment inoculated with these isolates. Because of their lower abundance in the samples, no significance was observed. The red vectors on the ordination plot represent the significant ($P < 0.01$) external variables that were implemented in the NMDS analysis (Table 1). Both helvolic acid and cerulenin production in the rice sheath and *in vitro* are characteristics of the *S. oryzae* isolates that significantly structure the community (Fig. 2).

Direct biotic interactions: dual plate assay

The bacteria that showed a significant non-random distribution (Pairs analysis) were used to further study the underlying biotic interactions. For this, the bacteria were co-cultured with *S. oryzae* isolates. According to the NMDS analysis, to which the helvolic acid and cerulenin production on PDA was projected as external variables, the *in vitro* toxin production of the *S. oryzae* isolates is a property that has a significant effect on the bacterial endophyte community (Fig. 2). As shown by the NMDS plot, the *in vitro* helvolic acid production differs from the production *in planta* which can be attributed to the instability of the helvolic acid production of *S. oryzae* isolate, RFNG41 (Table 1). While its helvolic acid production is very low *in planta*, the production *in vitro* is more stable and can reach the same levels as the virulent isolates (IBNG0008 and BDNG0025).

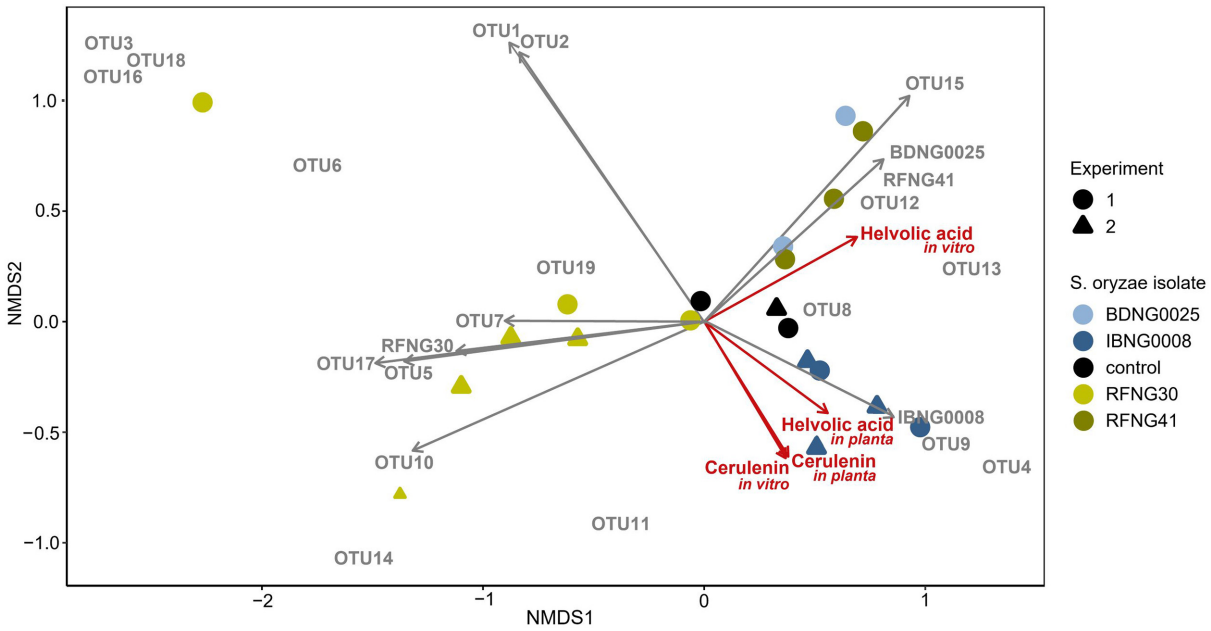

Figure 2. Non-metric multi-dimensional scaling (NMDS) ordination plot of the bacterial endophyte community in sheath rot infected plants. The ordination plot shows the individual samples, represented by symbols, together with the different operational taxonomic units (OTU's) and *S. oryzae* isolates that where collected from these samples. The colors of the symbols represent the treatment of the samples. The grey vectors on the plot show the intrinsic species score species that significantly ($P < 0.01$) correlate to the ordination and the red vectors show the significant ($P < 0.01$) external environmental factors.

Table 2. Pairs co-occurrence of *S. oryzae* isolates and the operational taxonomic units (OTUs) that were isolated from the rice sheaths.

S. oryzae isolate	OTU	Abundance [a] *S. oryzae* isolate	Abundance [a] OTU	Co-occurrence [b]	C-score*	*P*-value
IBNG0008	5	9	7	0	2.890	0.004
IBNG0008	7	9	10	0	3.738	< 0.001
IBNG0008	17	9	6	0	2.272	0.022
S. oryzae isolate	**OTU**	**Abundance S. oryzae isolate**	**Abundance OTU**	**Co-occurrence**	**T-score***	***P*-value**
RFNG30	5	9	7	7	3.769	< 0.001
RFNG30	7	9	10	8	3.693	< 0.001
RFNG30	10	9	4	4	2.123	0.033
RFNG30	17	9	6	6	4.357	< 0.001

[a]The number of samples from which the species was isolated.
[b]The number of samples from which both species were isolated.
*The values are the observed C-score or T-score that where sequentially Z-transformed and corrected following the BY-criterion.

The dual plate assay showed that the bacteria of OTU 7 interacted with *S. oryzae* in a helvolic acid-dependent way. When co-cultured with isolates that produce no helvolic acid (RFRG2 and RFNG30), the bacteria of OTU 7 were not inhibited while inhibition zones were observed when grown together with the helvolic acid producers (BDNG0025, IBNG0008 and RFRG41; Fig. 3 and Table 3). Compared to control plates without bacteria, all fungal isolates showed impaired growth when co-cultured with OTU 7 (Figs 3 and 4). Depending on the isolate, *S. oryzae* stopped growing or tried to avoid the bacterial streaks (Fig. 3). Microscopy revealed that the bacteria of OTU 7 accumulated on the hypha of *S. oryzae* in the interaction zone, leading to hyphal lysis and fragmentation (Fig. 3). Bacteria of the OTUs 5, 10 and 17 showed no growth inhibition when co-cultured with *S. oryzae* (Table 3). Colonies of the *S. oryzae* isolates RFNG30, RFNG41 and IBNG0008 were significantly smaller when grown with the OTUs 5 and 17 but the fungal colonies were not harmed (Fig. 4 and Table S8, Supporting Information). The presence of OTU 10 did not affect fungal growth (Fig. 4 and Table S8, Supporting Information).

Total and *Bacillus cereus* population densities in the presence of *S. oryzae*

Diversity analysis showed that infection of rice sheaths by *S. oryzae* isolates with no or low helvolic acid production *in planta* (RFNG30 and RFNG41) increased the diversity of the culturable bacteria. Rice sheaths infected by helvolic acid producers, IBNG0008 and BDNG0025, had a comparable Shannon index as healthy rice plants although species composition differed (Figs 1,and 2). Based on the statistical co-occurrence analysis, we revealed that the OTUs 5, 7, 10 and 17 aggregated with the isolate RFNG30 and further microscopic analysis indicated that the aggregation between OTU 7 and RFNG30 could be the result of direct biotic interaction (Table 2 and Fig. 3).

To confirm the statistical analysis, we quantified the total bacterial endophyte community and the *B. cereus* (OTU 7) population in plants at 11 days after inoculation with *S. oryzae* isolates that varied in virulence (Figure S1c, Supporting Information). To confirm the colonization by the fungus, sheath samples were plated on PDA. In all samples containing the edge of

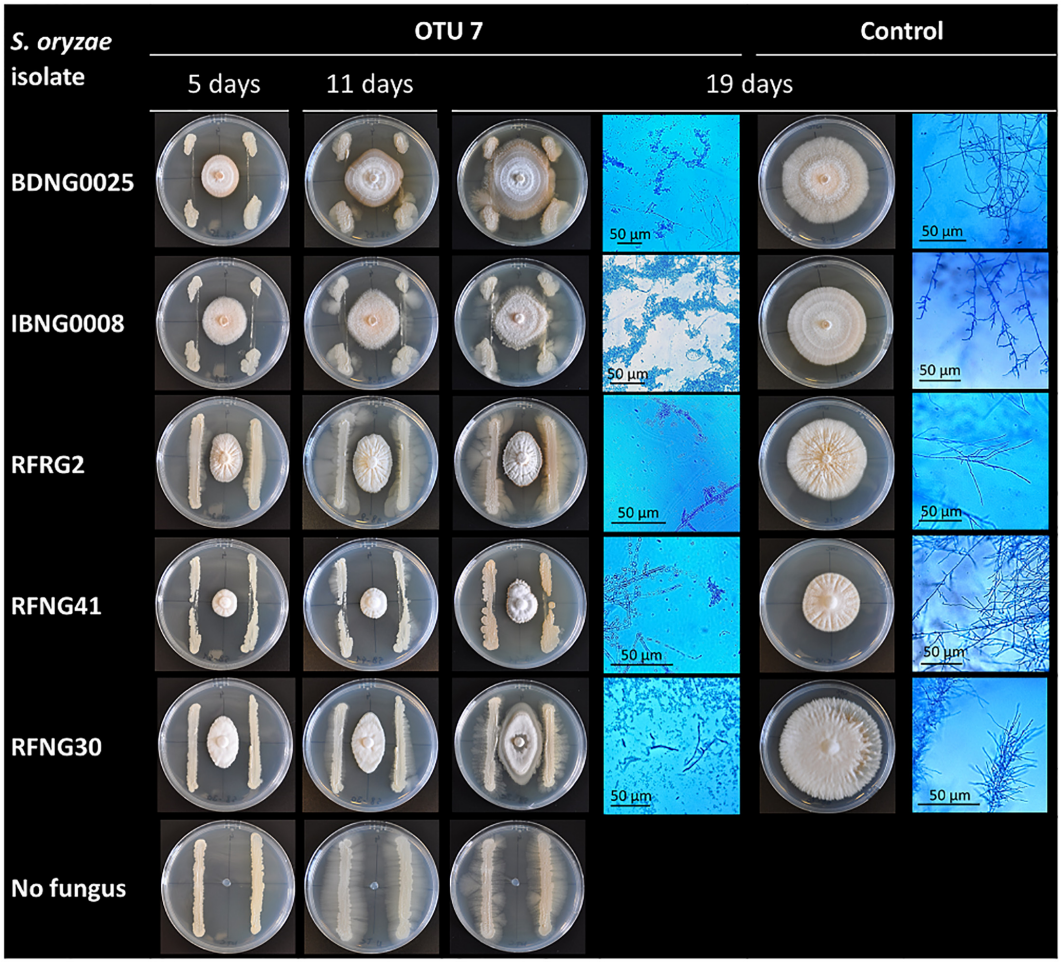

Figure 3. Pictures of a dual plate assay of *S. oryzae* isolates with isolate A-0–2 (OTU 7) and microscopic images of the interaction zone. The pictures were taken after 5, 11 and 19 days of co-incubation. After 19 days, the agar block smear technique was used to study the biotic interaction in the interaction zone. Agar blocks were stained with lactophenol cotton blue.

Table 3. Bacterial inhibition in a dual plate assay of *S. oryzae* with bacterial isolates belonging to the operational taxonomic units (OTU's) that were shown to have a non-random distribution. After 5 days of co-incubation, three levels of bacterial inhibition were scored; no inhibition (-), little inhibition (+) and strong inhibition (++).

			S. oryzae isolate				
Species (group)	OTU	Bacterial isolate	RFRG2	RFNG30	RFNG41	BDNG0025	IBNG0008
Bacillus megaterium	5	B-30-M	-	–	-	-	-
Bacillus cereus	7	A-0–2	–	–	+	++	++
Bacillus cereus	7	A-30–5	–	–	+	++	++
Bacillus cereus	7	A-41–3	–	–	+	++	++
Bacillus cereus	7	A-30–6	–	–	+	++	++
Bacillus cereus	7	B-30-X	–	–	+	++	++
Bacillus cereus	7	B-30-P	–	–	+	++	++
Brevibacillus nitrificans	10	B-30-D	–	–	-	-	-
Paenibacillus favisporus	17	B-30-L	–	–	-	-	-

the sheath rot lesion, the inoculated *S. oryzae* isolate was present while no fungus was isolated from the adjacent healthy sheath tissue. Comparison of the total amount of bacterial endophytes in the edge of the lesion containing necrotic tissue and adjacent healthy sheath tissue showed that the fungal inoculation method stimulated bacterial growth (Fig. 5A and C). Regardless of the fungal isolate, more bacteria were counted in the edge of the lesion than in the healthy sheath tissue. In these samples, the *B. cereus* population was quantified too (Fig. 5B). This showed that the majority of the isolated bacteria, represented in Fig. 5A, belongs to the *B. cereus* complex. For the isolates RFRG2, RFNG30 and RFNG41, *B. cereus* densities were higher in the necrotic tissue than in healthy sheath tissue but for plants infected by the toxin producer (IBNG0008), *B. cereus* densities had decreased (Fig. 5B).

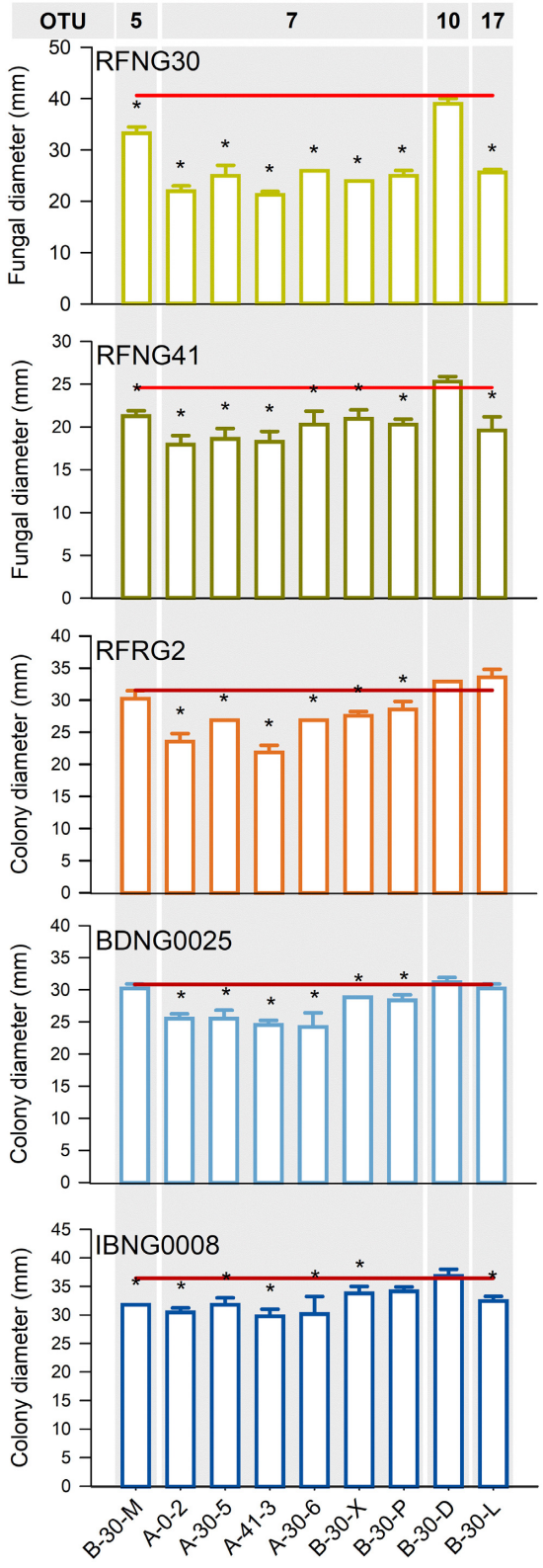

Figure 4. Colony diameter (mm) of 7 days old *S. oryzae* cultures on PDA after 5 days of co-incubation in a dual plate assay with bacterial isolates of the OTU's 5, 7, 10 and 17. All bars show the mean ± SD fungal colony diameter perpendicular to the bacterial streaks on both sides of the colony. The red line shows the mean colony diameter of the fungal isolate when grown on a plate without bacteria (control). Bars marked with an asterisk differ significantly from the control (type II ANOVA, $n = 3$, $\alpha = 0.05$).

In a repeat experiment, a second toxin-producing *S. oryzae* isolate (BDNG0025) was added to verify if the decline of the *B. cereus* population could be correlated to helvolic acid as indicated by the NMDS analysis and the dual plate assay (Fig. 2, Tables 2 and 3). This isolate produces high levels of helvolic acid but only low levels of cerulenin. The co-occurrence analysis showed that, of the culturable fraction, Gram-positive, spore-forming bacteria are the most affected by sheath rot infection. To study the trends in this bacterial sub-community, we repeated the experiment and heated the samples to kill non-spore forming bacteria. The unheated bacterial suspension was spread on two media, KB and R2A, and the heated suspension was plated on KB, R2A and MYP agar plates. The latter was added to confirm the *B. cereus* counts because this species shows a unique morphology on MYP selective agar (Fricker, Reissbrodt and Ehling-schulz 2008). It was confirmed statistically that both the total counts and the *B. cereus* counts of the heated and non-heated samples were the same on the different media, indicating that the results could be pooled for further analysis (Figure S4, Supporting Information). Figure 6 shows that the total amount of bacteria was the same in healthy rice sheaths and in the edge of lesions caused by the toxin-producing *S. oryzae* isolate (IBNG0008) and that samples of both conditions did not contain spores after heating. However, the samples did not contain the same bacteria. For the healthy sheaths, the amount of *B. cereus* colonies did not differ significantly from the total amount of bacteria while in the IBNG0008-infected plants no *B. cereus* was detected at all (Fig. 6A). The bacterial community of rice sheaths infected by *S. oryzae* BDNG0025, which produces high levels of helvolic acid and low levels of cerulenin, had a higher density and contained mostly spore-forming bacteria but no *B. cereus* (Fig. 6A and B). The densest populations were found in rice sheaths infected by lowest toxin-producers (RFNG30 or RFNG4) with *B. cereus* as the dominant species (Fig. 6A). The samples contained the highest number of spore-forming bacteria too and these were mostly *B. cereus* (Fig. 6B). Rice plants infected with an *S. oryzae* isolate that produced high levels of cerulenin but no helvolic acid (RFRG2), had a lower bacterial and spore density and contained mainly *B. cereus* and *B. cereus* spores (Fig. 6A and B).

DISCUSSION

This study investigated how *S. oryzae* affects the rice culturable bacterial endophyte community and with what interactions this pathogen needs to cope during infection. We started with characterizing the culturable bacterial endophytes in the edge of sheath rot lesions at tillering stage. The bacterial endophyte community of the healthy control plants was dominated by bacteria of the *B. cereus* group. The majority of the bacteria isolated from sheath rot lesions were Gram-positive bacteria, belonging to the genera *Bacillus*, *Paenibacillus* and *Brevibacillus*. Rice endophyte communities at tillering stage have been reported to be dominated by *Bacillus* spp. and shift to a community with mainly Gram-negative bacteria after flowering (Mano *et al.* 2007; Ren *et al.* 2015; Bertani *et al.* 2016). This indicates that the young age of the plants in this study could explain why very few Gram-negative bacteria were found. Next to growth stage (Mano *et al.* 2007; Yang *et al.* 2008; Bertani *et al.* 2016), other factors such as soil type (Hardoim *et al.* 2012) and the environmental conditions (Ren *et al.* 2015; Vacher *et al.* 2016; Venkatachalam *et al.* 2016) influence the endophyte community explaining the variation among studies.

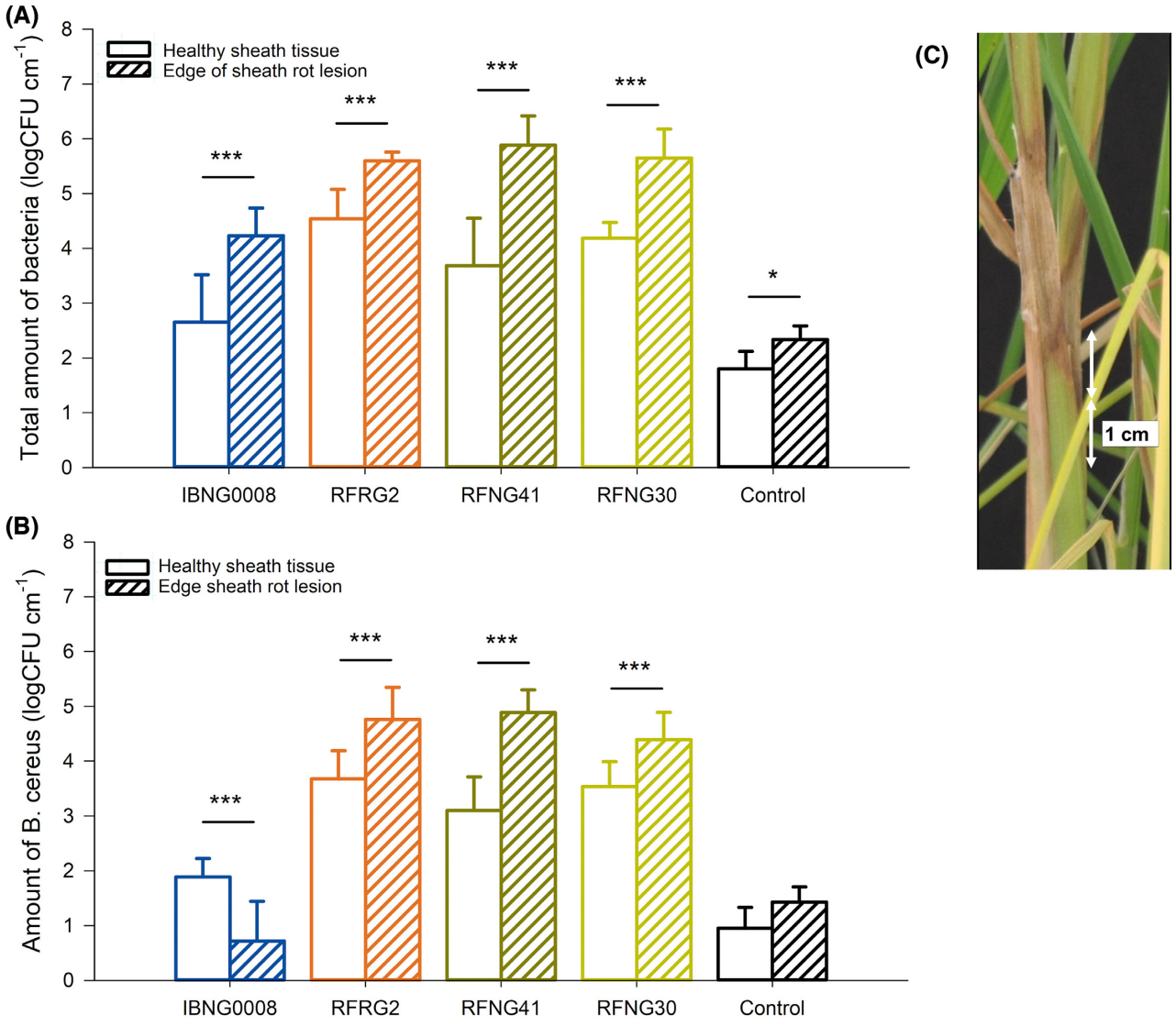

Figure 5. Counts (logCFU/cm) of the total culturable bacterial endophytes **(A)** and the Bacillus cereus population **(B)** in the edge of sheath rot lesions caused by *S. oryzae* isolates and in the adjacent healthy sheath tissue **(C)**. Rice plants cv Kitaake were inoculated with *S. oryzae* isolate IBNG0008 (dark blue), RFRG2 (orange), RFNG41 (dark green) and RFNG30 (light green) and sheath tissue was collected after 8 days of incubation. As a control, plants were inoculated with a sterile rice grain (black). A bacterial extract was plated on R2A and counted after 2 days of incubation (LOD = 1.2 CFU/cm). Bars show the mean counts ± SD, significant differences are marked with an asterisk (type III ANOVA, $n = 18$, $P < 0.05$; **, $P < 0.01$; ***, $P < 0.001$).

A previous study compared the pathobiome of healthy and sheath rot diseased plants in field conditions. They found a minor increase in diversity in plants infected by *Sarocladium* (Musonerimana *et al.* 2020). In this study, we found that the bacterial endophyte community in the edge of lesions of the two most virulent isolates had a similar Shannon index as the ones of the healthy sheath tissue. Identification of the isolated bacteria revealed that the communities strongly differed in structure at the species level. Lesions caused by the least virulent isolates harbored a more diverse bacterial endophyte community. It has been reported before that symptomless colonization of plants by pathogens results in a more diverse bacterial community. Like in the uninfected rice endosphere, the rhizosphere of uninfected avocado roots was reported to be colonized by a few predominant species. When avocado plants were infected with *Phytophthora cinnamomi* but did not show symptoms yet, the rhizosphere harbored a more diverse community with a very distinct structure (Yang, Crowley and Menge 2001). Moreover, Reiter *et al.* (2002) reported a more variable endophyte community in *Pectobacterium carotovorum*-infected but healthy potato plants compared to control plants. As a great portion of the isolated bacteria could protect potato plants from this pathogen, they suggest that the diverse endophyte community contributes to disease resistance (Reiter *et al.* 2002).

We found an enrichment of the *B. cereus* complex, the *Bacillus megaterium* complex, *Brevibacillus nitrificans* and *Paenibacillus favisporus* in the edge of the lesions of the least virulent, non-toxin producing *S. oryzae* isolate. These species co-occurred significantly with this *S. oryzae* isolate and they were eliminated by the virulent, helvolic acid-producing *S. oryzae* isolate. Co-culturing of the *B. megaterium*, *B. nitrificans* and *P. favisporus* isolates with *Sarocladium* showed that none of the *S. oryzae* isolates affected their growth (Table S8, Supporting Information). Moreover, some of the *S. oryzae* isolates showed a reduced growth rate in the presence of *B. megaterium* and *P. favisporus* isolates but these bacteria did not proliferate on the hypha or cause any damage. The

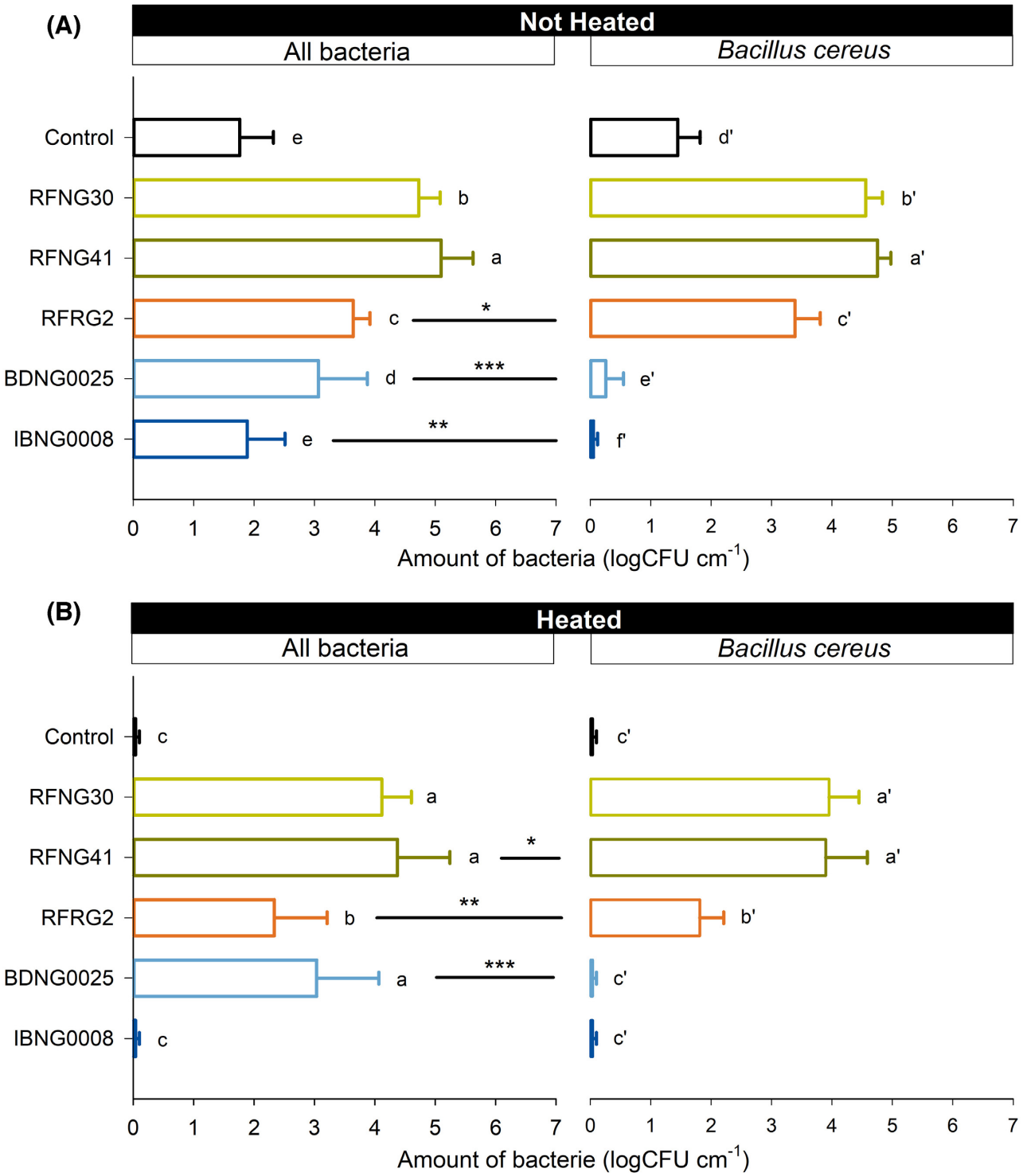

Figure 6. Counts (logCFU/cm) of the total culturable bacterial endophytes and the Bacillus cereus population in the edge of sheath rot lesions caused by *S. oryzae* isolates before **(A)** and after **(B)** heat treatment of the bacterial solution. Rice plants cv Kitaake were inoculated with *S. oryzae* isolate IBNG0008 (dark blue), BDNG0025 (light blue), RFRG2 (orange), RFNG41 (dark green) and RFNG30 (light green) and sheath tissue was collected after 8 days of incubation. As a control, plants were inoculated with a sterile rice grain (black). A bacterial extract was plated on KB, R2A and MYP agar and counted after 2 days of incubation (LOD = 1.3 CFU/cm). Counts of the three media were pooled and bars show the mean ± SD, significant differences are marked with an asterisk (Wilcoxon rank-sum test or two-sample *t*-test, $18 \leq n \leq 27$, $P < 0.05$; **, $P < 0.01$; ***, $P < 0.001$) or with different letters (type II ANOVA or Dunn test, posthoc Bonferroni, $18 \leq n \leq 27$).

enrichment can thus not be attributed to direct interactions with *S. oryzae* but is probably the result of indirect effects such as facilitation through the mobilization of nutrients towards the infection site and the release of cell content. This improves the conditions in the otherwise nutrient-poor environment, attracting and stimulating endophytes (Reiter *et al.* 2002) and epiphytes. This could also explain the enrichment of *B. cereus* since this bacterium grows well in sucrose-rich conditions such as in seeds, where it is found as the dominant species (Okunishi *et al.* 2005). However, *B. cereus* seems to interact directly with *S. oryzae*. All *S. oryzae* isolates showed impaired growth and, to a greater or lesser extent, hyphal lysis. The bacterium was strongly inhibited when co-cultured with helvolic acid-producing *S. oryzae* isolates while the *S. oryzae* isolate that produces no toxins did not affect *B. cereus* growth. Moreover, *B. cereus* colonized the hypha, causing severe damage. *B. cereus* produces various cell wall degrading enzymes such as chitinases, proteases and β-1,3-glucanases (Pleban, Chernin and Chet 1997; Singh *et al.* 2014). It had been shown to affect mycelial growth of various fungi such as *Fusarium oxysporum* and *Macrophomina phaseolina* (Singh *et al.* 2014), to inhibit *Fusarium oxysporum f. sp. meloni* spore germination and to protect cotton plants against *Rhizoctonia solani* (Pleban, Chernin and Chet 1997). Scanning electron microscopy showed *Bacilli* proliferating on fungal mycelium and destructing hypha (Singh *et al.* 2014).

Since *S. oryzae* is a slow grower (Bigirimana *et al.* 2015), it is not able to flee from antagonist so instead of avoiding competition, they need a defence mechanism (Gloer 1995). The production of helvolic acid seems to be effective in preventing *B. cereus* from causing damage as, in the presence of all helvolic acid producers, we observed inhibition zones and the bacterium was eliminated in the rice sheath. Cerulenin also seems to play a role in the interaction with the bacterial endophyte community. The virulent *S. oryzae* isolates, both produce high levels of helvolic acid which is correlated with their virulence (Peeters *et al.* 2020) but their cerulenin production varies. In rice sheaths infected by the helvolic acid-producer that makes only small amounts of cerulenin, spore-formers other than *B. cereus* were found. This illustrates the effect of the *S. oryzae* toxins on the community structure by creating a niche for toxin-resistant species with each having their characteristics such as antibiotic production, phytotoxicity or plant growth promotion.

Based on the fact that *S. oryzae* belongs to a genus that comprises mainly endophytes and opportunistic pathogens, we propose the idea that *S. oryzae* originates from an endophytic ancestor (Yeh and Kirschner 2014; Liu 2017; Anjos *et al.* 2020). The results of this study show that the production of antimicrobial compounds generates a competitive advantage to *S. oryzae* during the interaction with the host endophytes. Pathogens that are not able to withstand negative biotic interaction are predicted to have a reduced colonization success and virulence too. The production of antibiotics and other defence mechanisms against microbes is an important trait of pathogens that could be the target of control measures. Moreover, these traits should be taken into account in the search for biocontrol measures. The diversity of the pathogen population should be considered and its interaction with the pathobiome should be understood. In the case of *S. oryzae*, we advise to include various *S. oryzae* isolates and characterize their toxin production *in vitro* and *in planta* since these toxins determine the outcome of the interaction with the candidate biocontrol organisms. Moreover, the stability of the toxin production is determined by the phenotypic stability which is on its turn related to the phylogeny (Peeters *et al.* 2020). It is thus important to define to which group the used *S. oryzae* isolate belongs. A recent study even appointed these three lineages as three distinct species, namely *S. sparsum* (Group 3), *S. attenuatum* (Group 2) and *S. oryzae* (Group 1; Table 1; Ou, Lin and Chen 2020) which could indicate that these *S. oryzae* lineages differ in many more characteristics, stressing the need for exhaustive characterization of the isolates used for research. As these species are closely related and all cause rice sheath rot, we propose to classify them in the *S. oryzae* species complex.

Preliminary results indicate that *S. oryzae* isolates that lack toxin production are impaired in their colonization. This should be confirmed in future research. Moreover, the helvolic acid production of endophytes should be studied during host colonization to verify if they produce the toxin *in planta* and if they do, why the toxin has no phytotoxic effect in this case. It would also be interesting to investigate if the diverse endophyte community attributes to the increased resistance.

ACKNOWLEDGMENTS

We would want to thank the lab technicians Nadia Lemeire and Ilse Delaere for the help in the lab. Also special thanks to the glasshouse responsible Stefan Vidts. The graphical abstract was created with BioRender.com.

SUPPLEMENTARY DATA

Supplementary data are available at *FEMSEC* online.

FUNDING

This work was supported by the Fund for Scientific Research-Flanders (FWO; grant number G031317N).

Conflicts of interest. None declared.

REFERENCES

Anjos RM, Moreira SI, Costa SS *et al. Sarocladium graminicola*, a new endophytic species from tropical grasses. *Mycol Prog* 2020;**19**:605–14.

Ardanov P, Ovcharenko L, Zaets I *et al.* Endophytic bacteria enhancing growth and disease resistance of potato (*Solanum tuberosum* L.). *Biol Control* 2011;**56**:43–9.

Ayyadurai N, Kirubakaran S, Srisha S *et al.* Biological and molecular variability of *Sarocladium oryzae*, the sheath rot pathogen of rice (*Oryza sativa* L.). *Curr Microbiol* 2005;**50**:319–23.

Bacon CW, Hinton DM. Bacterial endophytes: the endophytic niche, its occupants, and its utility. *Plant Assoc Bact* 2006:155–94, DOI: 10.1007/978-1-4020-4538-7_5.

Bates D, Mächler M, Bolker BM *et al.* Fitting linear mixed-effects models using lme4. *J Stat Softw* 2015;**67**, DOI: 10.18637/jss.v067.i01.

Bertani I, Abbruscato P, Piffanelli P *et al.* Rice bacterial endophytes: Isolation of a collection, identification of beneficial strains and microbiome analysis. *Environ Microbiol Rep* 2016;**8**:388–98.

Bigirimana V, Hua G, Nyamangyoku O *et al.* Rice sheath rot: an emerging ubiquitous destructive disease complex. *Front Plant Sci* 2015;**6**:1–28.

Brusini J, Robin C. Mycovirus transmission revisited by in situ pairings of vegetatively incompatible isolates of *Cryphonectria parasitica*. *J Virol Methods* 2013;**187**:435–42.

CABI. Sarocladium oryzae (rice sheath rot) & *Pseudomonas fuscovaginae* (sheath brown rot). *datasheet* 48393, 44957 (8 June

2020, date last accessed). https://www.cabi.org/isc/datasheet/48393, https://www.cabi.org/isc/datasheet/44957.

Coraiola M, Paletti R, Fiore A *et al.* Fuscopeptins, antimicrobial lipodepsipeptides from *Pseudomonas fuscovaginae*, are channel forming peptides active on biological and model membranes. *J Pept Sci* 2008;**14**:496–502.

Cottyn B, Debode J, Regalado E *et al.* Phenotypic and genetic diversity of rice seed-associated bacteria and their role in pathogenicity and biological control. *J Appl Microbiol* 2009;**107**:885–97.

Deveau A, Bonito G, Uehling J *et al.* Bacterial-fungal interactions: ecology, mechanisms and challenges. *FEMS Microbiol Rev* 2018;**42**:335–52.

Dinno A., *Package Dunn.Test: Dunn's Test of Multiple Comparisons Using Rank Sums*, CRAN R Package Version 1.3.5. 2017.

Duffy B, Schouten A, Raaijmakers JM. Pathogen self-defense: mechanisms to counteract microbial antagonism. *Annu Rev Phytopathol* 2003;**41**:501–38.

Dugay FD, Manandhar JB, Mew TW. Transmissibility of *Sarocladium oryzae* (SAWADA) from the seed to the seedling, *Philippine Phytopathol* 1996; **32**:130–1.

Edgar RC. MUSCLE: multiple sequence alignment with high accuracy and high throughput. *Nucleic Acids Res* 2004;**32**:1792–7.

Elbeltagy A, Nishioka K, Suzuki H *et al.* Isolation and characterization of endophytic bacteria from wild and traditionally cultivated rice varieties. *Soil Sci Plant Nutr* 2000;**46**:617–29.

Fox J, Weisberg S. *An {R} Companion to Applied Regression*. 3rd ed. Sage, 2019.

Fricker M, Reissbrodt R, Ehling-schulz M. Evaluation of standard and new chromogenic selective plating media for isolation and identification of *Bacillus cereus*. *Int J Food Microbiol* 2008;**121**:27–34.

Ghosh M, Amudha R, Jayachandran S *et al.* Detection and quantification of phytotoxic metabolites of *Sarocladium oryzae* in sheath rot-infected grains of rice. *Lett Appl Microbiol* 2002;**34**:398–401.

Giraldo A, Gené J, Sutton D *et al.* Phylogeny of *Sarocladium* (Hypocreales). *Persoonia* 2015;**34**:10–24.

Gloer JB. The chemistry of fungal antagonism and defense. *Can J Bot* 1995; **73**:1265–74.

Gotelli N, Hart E, Ellison A. Null model analysis for ecological data. *R Package* Version 0.1.0 2015.

Hardoim PR, Hardoim CCP, van Overbeek LS *et al.* Dynamics of seed-borne rice endophytes on early plant growth stages. *PLoS One* 2012;**7**, DOI: 10.1371/journal.pone.0030438.

Helsel DR. *Nondectects and Data Analysis; Statistics for Censored Environmental Data*. USA, NJ: John Wiley and Sons, 2005.

Hittalmani S, Mahesh H, Mahadevaiah C *et al.* De novo genome assembly and annotation of rice sheath rot fungus *Sarocladium oryzae* reveals genes involved in helvolic acid and cerulenin biosynthesis pathways. *BMC Genom* 2016;**17**:1–13.

Jakuschkin B, Fievet V, Schwaller L *et al.* Deciphering the pathobiome: Intra- and interkingdom interactions involving the pathogen *Erysiphe alphitoides*. *Microb Ecol* 2016;**72**:870–80.

King EO, Ward MK, Raney DE. Two simple media for the demonstration of pyocyanin and fluorescin. *J Lab Clin Med* 1954;**44**:301–30.

Kombrink A, Thomma B. LysM Effectors: secreted proteins supporting fungal life. *PLoS Pathog* 2013;**9**:1–4.

Laforest-Lapointe I, Paquette A, Messier C *et al.* Leaf bacterial diversity mediates plant diversity and ecosystem function relationships. *Nature* 2017;**546**:145–7.

Lenth R. *Emmeans: Estimated Marginal Means, Aka Least-Squares Means*, R Package Version 1.4.6, 2020.

Liu X. *Sarocladium brachiariae* sp. nov., an endophytic fungus isolated from *Brachiaria brizantha*. *Mycosphere* 2017;**8**:827–34.

Mano H, Morisaki H. Endophytic bacteria in the rice plant. *Microbes Environ* 2008;**23**:109–17.

Mano H, Tanaka F, Nakamura C *et al.* Culturable endophytic bacterial flora of the maturing leaves and roots of rice plants (*Oryza sativa*) cultivated in a paddy field. *Microbes Environ* 2007;**22**:175–85.

Musonerimana S, Bez C, Licastro D *et al.* Pathobiomes revealed that *Pseudomonas fuscovaginae* and *Sarocladium oryzae* are independently associated with rice sheath rot. *Microb Ecol* 2020, DOI: 10.1007/s00248-020-01529-2.

Nuss DL. Hypovirulence: mycoviruses at the fungal-plant interface. *Nat Rev Microbiol* 2005;**3**:632–42.

Oksanen J, Blanchet FG, Friendly M *et al.* Package "vegan": community ecology package. *Community Ecol Package* 2019;**2**:1–297.

Okunishi S, Sako K, Mano H *et al.* Bacterial flora of endophytes in the maturing seed of cultivated rice (*Oryza sativa*). *Microbes Environ* 2005;**20**:168–77.

Omura S. The antibiotic cerulenin, a novel tool for biochemistry as an inhibitor of fatty acid synthesis. *Bacteriol Rev* 1976;**40**:681–97.

Ou JH, Lin GC, Chen CY. *Sarocladium* species associated with rice in Taiwan. *Mycol Prog* 2020;**19**:67–80.

Panda KK, Mishra MK. Studies on physiological characteristics of *Sarocladium oryzae* causing sheath rot of rice. *Int J Curr Microbiol App Sci* 2019;**8**:1767–74.

Pearce DA, Bridge PD, Hawkworth DL. Species concept in *Sarocladium*, the causal agent of sheath rot in rice and bamboo blight. *Major Fung Dis Rice Recent Adv*. 2001:285–92, DOI: 10.1007/978-94-017-2157-8_20.

Peeters KJ, Haeck A, Harinck L *et al.* Morphological, pathogenic and toxigenic variability in the rice sheath rot pathogen *Sarocladium oryzae*. *Toxins* 2020;**12**:1–17.

Pleban S, Chernin L, Chet I. Chitinolytic activity of an endophytic strain of *Bacillus cereus*. *Lett Appl Microbiol* 1997;**25**:284–8.

Porrini L, Cybulski LE, Altabe SG *et al.* Cerulenin inhibits unsaturated fatty acids synthesis in *Bacillus subtilis* by modifying the input signal of DesK thermosensor. *Microbiologyopen* 2014;**3**:213–24.

Ratnaweera P, Williams D, de Silva E *et al.* Helvolic acid, an antibacterial nortriterpenoid from a fungal endophyte, *Xylaria sp.* of orchid *Anoectochilus setaceus* endemic to Sri Lanka. *Mycology* 2014;**5**:23–8.

R Core Team. *R: A Language and Environment for Statistical Computing*. Vienna, Austria, 2020.

Reiter B, Pfeifer U, Schwab H *et al.* Response of endophytic bacterial communities in potato plants to infection with *Erwinia carotovora subsp. atroseptica*. *Appl Environ Microbiol* 2002;**68**:2261–8.

Ren G, Zhu C, Alam MS *et al.* Response of soil, leaf endosphere and phyllosphere bacterial communities to elevated CO2 and soil temperature in a rice paddy. *Plant Soil* 2015;**392**:27–44.

Rovenich H, Boshoven JC, Thomma B. Filamentous pathogen effector functions: of pathogens, hosts and microbiomes. *Curr Opin Plant Biol* 2014;**20**:96–103.

Sakthivel N, Amudha R, Muthukrishnan S. Production of phytotoxic metabolites by *Sarocladium oryzae*. *Mycol Res* 2002;**106**:609–14.

Sakthivel N, Gnanamanickam SS. Evaluation of *Pseudomonas fluorescens* for suppression of sheath rot disease and for

enhancement of grain yields in rice (*Oryza sativa* L.). *Appl Environ Microbiol* 1987;**53**:2056–9.

Sakthivel N. *Sheath rot disease of rice: current status and control strategies*. In: Sreenivasaprasad S, Johnson R (eds.). Major Fungal Diseases of Rice: Recent Advances. Pondicherry University: Kluwer Academic Publishes, 2001, 271–83.

Santos V, Mascarin GM, da Silva Lopes M *et al.* Identification of double-stranded RNA viruses in Brazilian strains of *Metarhizium anisopliae* and their effects on fungal biology and virulence. *Plant Gene* 2017;**11**:49–58.

Singh RK, Kumar DP, Singh P *et al.* Multifarious plant growth promoting characteristics of chickpea rhizosphere associated *Bacilli* help to suppress soil-borne pathogens. *Plant Growth Regul* 2014;**73**:91–101.

Singmann H, Bolker B, Westfall J *et al. Afex: Analysis of Factorial Experiments*, R Package Version 0.27-2, 2020.

Sreenivasaprasad S, Johnson R. (eds.). *Major Fungal Diseases of Rice: Recent advances*, Springer Science & Business Media. 2001.

Tamura K, Stecher G, Peterson D *et al.* MEGA6: molecular evolutionary genetics analysis version 6.0. *Mol Biol Evol* 2013;**30**:2725–9.

Tanaka N, Kinoshita T, Masukawa H. Mechanism of inhibition of protein synthesis by fusidic acid and related steroidal antibiotics. *J Biochem* 1969;**65**:459–64.

Tschen J, Chen L, Hsieh S *et al.* Isolation and phytotoxic effects of helvolic acid from plant pathogenic fungus *Sarocladium oryzae*. *Bot Bull Acad Sinica* 1997;**38**:251–6.

Ulrich W. *Pairs – a FORTRAN program for studying pairwise species associations in ecological matrices* 2008.

Vacher C, Hampe A, Porté AJ *et al.* The phyllosphere: microbial jungle at the plant–climate interface. *Annu Rev Ecol Evol Syst* 2016;**47**:1–24.

Vayssier-Taussat M, Albina E, Citti C *et al.* Shifting the paradigm from pathogens to pathobiome new concepts in the light of meta-omics. *Front Cell Infect Microbiol* 2014;**5**:1–7.

Venkatachalam S, Ranjan K, Prasanna R *et al.* Diversity and functional traits of culturable microbiome members, including cyanobacteria in the rice phyllosphere. *Plant Biol (Stuttg)* 2016;**18**:627–37.

Vorholt JA. Microbial life in the phyllosphere. *Nat Rev Microbiol* 2012;**10**:828–40.

Wenzel M, Patra M, Albrecht D *et al.* Proteomic signature of fatty acid biosynthesis inhibition available for in vivo mechanism-of-action studies. *Antimicrob Agents Chemother* 2011;**55**:2590–6.

Whipps JM. Microbial interactions and biocontrol in the rhizosphere. *J Exp Bot* 2001;**52**:487–511.

Woo PCY, Ngan AHY, Chui HK *et al.* Agar block smear preparation: a novel method of slide preparation for preservation of native fungal structures for microscopic examination and long-term storage. *J Clin Microbiol* 2010;**48**:3053–61.

Yakimov MM, Giuliano L, Gentile G *et al. Oleispira antarctica* gen. nov., sp. nov., a novel hydrocarbonoclastic marine bacterium isolated from Antarctic coastal sea water. *Int J Syst Evol Microbiol* 2003;**53**:779–85.

Yang CH, Crowley DE, Menge JA. 16S rDNA fingerprinting of rhizosphere bacterial communities associated with healthy and *Phytophthora* infected avocado roots. *FEMS Microbiol Ecol* 2001;**35**:129–36.

Yang JH, Liu HX, Zhu GM *et al.* Diversity analysis of antagonists from rice-associated bacteria and their application in biocontrol of rice diseases. *J Appl Microbiol* 2008;**104**:91–104.

Yaov B, Yekuteli D. The control of false discovery rate in multiple testing under dependency. *Ann Stat* 2001;**29**:1165–88.

Yeh YH, Kirschner R. *Sarocladium spinificis*, a new endophytic species from the coastal grass *Spinifex littoreus* in Taiwan. *Bot Stud* 2014;**55**:1–6.

Yoshimura F. Properties of membrane adenosine triphosphatase of the obligately anaerobic bacterium *Veillonella alcalescens*. *J Biochem* 1978;**83**:1231–8.